Macromolecules **2000,** *33,* 3739−3746

Linear Viscoelasticity of Disordered Polystyrene−Polyisoprene Block Copolymer Based Layered-Silicate Nanocomposites

Jiaxiang Ren, Adriana S. Silva, and Ramanan Krishnamoorti*

Department of Chemical Engineering, University of Houston, Houston, Texas 77204

Received December 14, 1999

ABSTRACT: The melt-state linear viscoelastic properties for a series of intercalated nanocomposites are examined. The nanocomposites are based on a short disordered polystyrene−polyisoprene diblock copolymer and varying amounts of dimethyldioctadecylammonium modified montmorillonite. The linear dynamic oscillatory moduli and the stress relaxation moduli are in quantitative agreement and suggest that at short times the relaxation of the nanocomposites is essentially unaffected by the presence of the layered-silicate. However, at long times (or equivalently low frequency), the hybrids exhibit dramatically altered viscoelastic behavior. Hybrids with silicate loadings in excess of 6.7 wt % exhibit pseudo-solidlike behavior, similar to that observed in previous studies of exfoliated end-tethered nanocomposites. On the basis of simple phenomenological arguments, the long time behavior is attributed to the presence of anisotropic stacks of silicate sheets randomly oriented and forming a percolated network structure that is incapable of relaxing completely. These arguments are further supported by the ability of large-amplitude oscillatory shear to orient these nanocomposites and to increase their liquidlike character.

Introduction

Layered-silicate-based polymer nanocomposites have attracted considerable technological and scientific interest during the recent past.[1−4] The technological interest has stemmed from the dramatic enhancements in physical, thermal, and mechanical properties of polymer-based materials with minimal increase in density due to the low inorganic loading required.[4] On the other hand, these materials have also proved to be model systems to examine the underlying molecular level underpinnings of the structure and dynamic properties of confined polymer systems and polymer brushes using macroscopic characterization techniques.[2,3] A significant possible impediment to the technological application of these materials relates to their processability. Further, a thorough understanding of the changes to the structure and properties by the processing conditions imposed is essential to tailor nanocomposite for specific applications.

Hybrids prepared by dispersion of similar organically modified layered silicates in small molecule organic solvents are commonly used in the paint and lubrication industry.[5] Rheological studies of these systems have suggested that the flow properties are highly irreproducible, with dramatic alterations to the structure by the imposition of even small-amplitude oscillatory shear.[6] On the other hand, the viscoelastic properties of intercalated and exfoliated layered-silicate-based nanocomposites have been reported recently.[2,3,7] The data reported showed little of the complexity traditionally associated with the small molecule analogues, and the differences are thought to be a result of the extent of dispersion of the silicate layers in the two cases. Further, significant changes in the viscoelastic properties depending on the mesoscopic structure and strength of polymer−layered-silicate interactions were observed. For intercalated poly(dimethyl-*co*-diphenylsiloxane)-based nanocomposites, alterations in the low-frequency (and low shear rate) behavior were observed.[3] Specifically, non-Newtonian viscosity behavior was observed at all silicate loadings, and the low-frequency storage modulus exhibited the development of a plateau. On the other hand, poly(dimethylsiloxane)-based exfoliated nanocomposites showed little changes in the viscoelastic properties with the exception of an increase in the modulus and viscosity with increased silicate content. In contrast, for exfoliated nanocomposites developed by *tethering* the chains to the layered-silicate (based on nylon-6 and poly(ϵ-caprolactone)), significant differences in the viscoelastic properties were observed.[7] The low-frequency storage and loss moduli gradually changed from liquidlike (for the polymers) to a pseudo-solidlike behavior for nanocomposites with as little as 3 wt % layered-silicate. These nanocomposites could be oriented by the application of large-amplitude oscillatory shear and thus exhibit enhanced low-frequency dependence of the linear viscoelastic moduli and highly unusual nonlinear viscoelastic properties.[7,8]

We have conducted an experimental investigation of the linear and nonlinear rheological properties for a model polymer−layered-silicate nanocomposite. Unlike the previous studies, a model monodisperse polymer was used here. In particular, a nearly symmetrical disordered diblock copolymer of polystyrene and 1,4-polyisoprene was chosen, with the expectation that only the polystyrene block would be attracted to the layered-silicate. The results of this paper, however, conclusively prove that the rheological properties are essentially unaffected by the detailed choice of the chemical nature of the polymer (i.e., block copolymer vs homopolymer) and are most crucially affected by the dispersion of the silicate layers. In this paper, we focus on the linear viscoelastic properties for these hybrids and will discuss the nonlinear properties and the transition from linear to nonlinear properties in a subsequent paper.[9]

Experimental Methods

An anionically synthesized monodisperse polystyrene−1,4-polyisoprene (7 mol % 3,4 and 93 mol % 1,4) diblock copolymer (PSPI18) was used in this study. It has a molecular weight

10.1021/ma992091u CCC: $19.00

M_w of 17 700 with $M_w/M_n < 1.07$, PS content of 44 wt %, and an order–disorder transition temperature below 80 °C (i.e., it is disordered for $T \geq 80$ °C). The layered-silicate used in this study was a montmorillonite with a charge exchange capacity (CEC) of 90 mequiv/100 g and organically modified with a dimethyldioctadecylammonium cation (2C18M). Excess alkylammonium ions were removed by repeatedly refluxing the organically modified layered-silicate with boiling ethanol. The amount of alkylammonium was found to be 26.8 wt % (by thermogravimetric analysis (TGA)), consistent with the known CEC of the silicate. TGA measurements performed on a Seiko TG/DTA 320 thermal analyzer were also used to verify the inorganic fraction in the pure 2C18M and nanocomposites. These measurements were conducted at a heating rate of 10 °C/min from room temperature to 500 °C and subsequent holding at 500 °C for half an hour under flowing air.

Nanocomposites were prepared by solution mixing appropriate quantities of finely ground 2C18M and PSPI18 in toluene at room temperature. Five hybrids with silicate contents of 0.7, 2.1, 3.5, 6.7, and 9.5 wt % were prepared for this study. The homogeneous solutions were dried extensively at room temperature and subsequently annealed at 100 °C in a vacuum oven for ~12 h to remove any remaining solvent and to facilitate complete polymer intercalation between the silicate layers.

X-ray diffraction was used to verify the gallery height and was performed using a Siemens D5000 X-ray diffractometer with Cu Kα radiation generated at 40 mA and 50 kV. Diffraction spectra were obtained over a 2θ range of 2°–10° in steps of 0.02° and counting times of 3 s at each angular position.

Rheological measurements were performed on a Rheometric Scientific ARES rheometer with a torque transducer capable of measurements over the range of 0.2–2000 g cm. Dynamic oscillatory shear measurements were performed using a set of 25 mm diameter parallel plates with a sample thickness of 1–2 mm and a temperature range of 80–105 °C. A sinusoidal strain of the form

$$\gamma(t) = \gamma_0 \sin(\omega t) \tag{1}$$

was applied, where γ_0 is the strain amplitude, ω is the frequency (varied from 0.001 to 100 rad/s), and t is the time. The resulting time dependence of the stress is

$$\sigma(t) = \gamma_0(G' \sin(\omega t) + G'' \cos(\omega t)) \tag{2}$$

where $\sigma(t)$ is the shear stress, G' is the storage or elastic modulus, and G'' is the loss or viscous modulus. The linear viscoelastic moduli reported here were ensured to be independent of the strain amplitude by repeat measurements using higher and lower strain amplitudes.

Stress relaxation measurements were performed at 85 °C using a 25 mm diameter cone and plate geometry with a cone angle of 0.0998 rad. A single step strain γ_0 was applied at time $t = 0$, and the shear stress $\sigma(t)$ was measured as a function of time, with the modulus $G(t)$ obtained as

$$G(t) = \frac{\sigma(t)}{\gamma_0} \tag{3}$$

The stress relaxation data reported in this paper were obtained at low strains and were verified to be in the linear regime.[9] Dynamic measurements of G' and G'' as a function of ω obtained at 85 °C with the parallel-plate and cone-and-plate geometry agreed to within 2% for all the samples.

Results and Discussion

a. Structure. X-ray diffraction spectra for the pure 2C18M and various representative hybrids are presented in Figure 1a. The interlayer gallery height, calculated as the difference of the d_{001} distance obtained by XRD and the individual layer thickness (0.95 nm), for the pure 2C18M is ~1.3 nm which, upon intercalation by polystyrene (PS, $M_w = 30$K) or PSPI18, expands to ~2.1 and 2.5 nm, respectively. However, the hybrids prepared with 1,4-polyisoprene (PI, $M_w = 17$K) showed no change in gallery spacing, indicative of the immiscibility of PI and 2C18M. The intercalation of 2C18M by PS and not by PI is consistent with the results of previous experimental work[10] and the theories of Vaia and Giannelis[11] and of Balazs and co-workers.[12] PS intercalates the interlayer galleries due to the slight Lewis base character imparted by the phenyl ring, leading to favorable interactions with the silicate layers.[13]

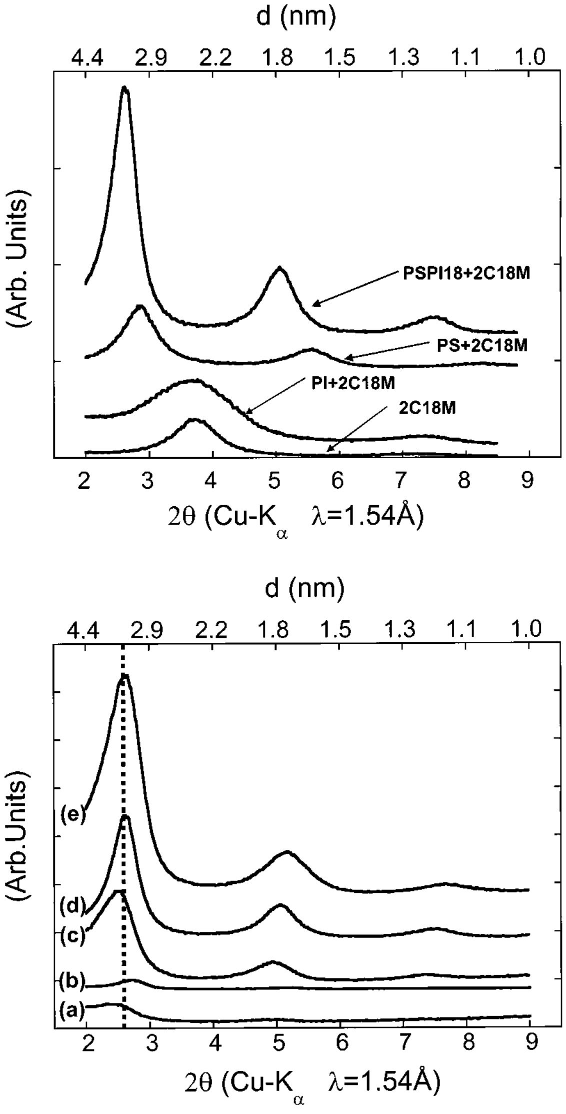

Figure 1. (a, top) X-ray diffraction spectra for pure 2C18M, PI + 2C18M, PS + 2C18M and PSPI18 + 2C18M hybrids. The d_{001} peaks for the 2C18M and PI + 2C18M are at similar locations, indicating that the PI does not intercalate the layered silicate. On the other hand, both the PS + 2C18M and PSPI18 + 2C18M hybrids exhibit expansion of the interlayer gallery spacing with the preservation of long-range order, seen by the presence of d_{002} and d_{003} peaks. The gallery height of PSPI18 + 2C18M is ~0.4 nm greater than that of the PS + 2C18M intercalated nanocomposites. (b, bottom) X-ray diffraction spectra for PSPI18 + 2C18M intercalated hybrids with silicate loadings (a) 0.7, (b) 2.1, (c) 3.5, (d) 6.7, and (e) 9.5 wt %. The location of the d_{001} peak is essentially unaffected by the increase in silicate loading.

Further, the interlayer gallery spacing for the PSPI18–2C18M hybrids is independent of the silicate loading, as evidenced from Figure 1b. All the hybrids exhibit clear regular layered structure, demonstrated by the presence of the d_{001} and higher-order diffraction peaks. This independence of the gallery height on silicate loading is consistent with the results of Vaia and coworkers on model PS-based nanocomposites.[10] A simple space filling calculation assuming the polymer density to be unaffected by confinement and with little or no exfoliation or disordering of the layers suggests that, for hybrids with more than 30 wt % polymer, there exists excess polymer that is not intercalated between the layers.

The increased gallery height for the PSPI18 intercalated nanocomposites, as compared to the PS-based hybrids, is noteworthy. This increased gallery height is attributed to the incorporation of the disfavored PI block in the interlayer galleries due to the preferential attraction of the PS block to the silicate surface and the connectivity imposed by the diblock architecture. Since the layers are two-dimensional ceramic sheets of ∼0.5−1 μm lateral dimensions, it would be virtually impossible to conceive a situation where the PS block, with an extended end-to-end distance of <50 nm, intercalates the interlayer galleries at the edges and excludes the PI from the intergallery region. Such a geometry, where the preferred PS block infiltrates the edges and expands the galleries, is impossible to sustain due to the large bending modulus of the ceramic sheets and van der Waals interactions, albeit weak, between the layers.[14] To sustain the long-range order of the layers evidenced in the XRD measurements would require the interlayer galleries to be completely filled by the polymer chains and would require the PI block to also enter the interlayer galleries. Thus, we suggest that the internal arrangement of PSPI18 within the gallery would have the PS block closer to both silicate surfaces (due to the preferential attraction) and the PI block occupying the central portion of the interlayer gallery.[15−17] This, however, does not imply that the internal polymer structure would be that of a crystalline solid, but rather a liquidlike structure.[18] Such a conformation would also be consistent with the increased gallery height for the PSPI18 nanocomposites as compared to that of the PS-based hybrids.

b. Melt Rheology. (i) Linear Dynamic Viscoelasticity. The linear dynamic viscoelastic master curves for the unfilled PSPI18 are shown in Figure 2. The master curves, generated by applying the principle of time−temperature superposition to isothermal frequency scans, were shifted to a common reference temperature (T_0) of 85 °C using both frequency shift factors (a_T) and modulus shift factors (b_T). The data, in this master curve and subsequent master curves discussed in this paper, were ensured to be in the linear regime by obtaining the same strain-independent viscoelastic properties using strain amplitudes 2-fold larger and smaller than the ones for which data are reported. Prolonged heating of the samples in the rheometer with flowing N_2 resulted in no change in the viscoelastic data. Additionally, gel permeation chromatography of the polymer after rheological testing exhibited no cross-linking or degradation.

On the basis of the molecular weight of PSPI18 and the known entanglement molecular weights of PS and PI ($M_{e,PS} = 18K$ and $M_{e,PI} = 5K$),[19] we expect PSPI18 to be lightly entangled. The data shown in Figure 2 are consistent with that of a lightly entangled polymer with pure liquidlike relaxation behavior (i.e., $G' \sim \omega^2$, and $G'' \sim \omega^1$) below $a_T\omega$ of ∼10 rad/s. For lightly entangled homopolymers, the longest relaxation time of the chains, τ, is obtained by extrapolating the G' and G'' vs ω lines (on a log−log plot) in the terminal region and locating ω_{int}, the value of ω where these lines intersect.[20] The value of τ lies between $2/\omega_{int}$ and $3/\omega_{int}$, depending on the extent of entanglement. We estimate the terminal relaxation time of the polymer chains to be between 0.2 and 0.3 s at 85 °C.

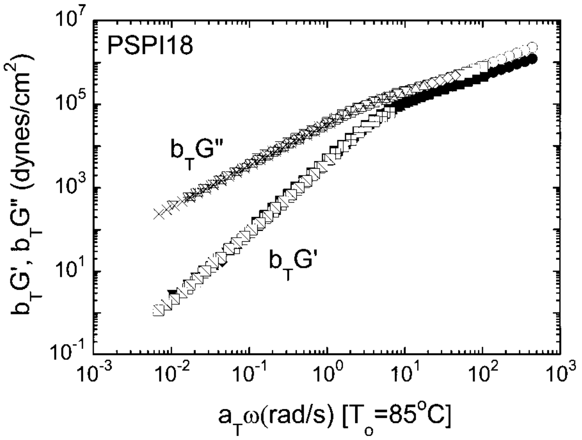

Figure 2. Time−temperature superposed linear viscoelastic dynamic moduli (storage modulus G' and loss modulus G'') for PSPI18. Frequency scans from 80 to 105 °C were superposed using frequency and moduli shift factors (a_T and b_T, respectively, shown in Figure 5).

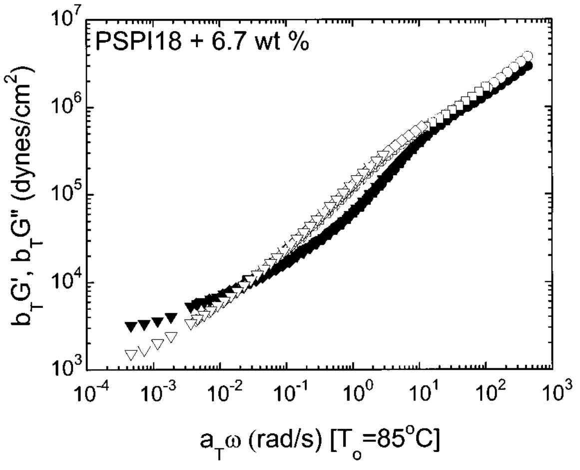

Figure 3. Time−temperature superposed linear viscoelastic moduli of a PSPI18 + 6.7 wt % 2C18M intercalated hybrid. Open symbols correspond to b_TG'' while the filled symbols correspond to b_TG'. The frequency and moduli shift factors are shown in Figure 5. A comparison with Figure 2 suggests that the high-frequency moduli are unaffected with the exception of increases in the magnitude of both the storage and loss moduli. However, at low frequency the frequency dependence of the moduli for the hybrid is distinctly different from that of PSPI18. The low-frequency behavior is consistent with that of a material exhibiting pseudo-solidlike behavior.

In contrast, the time−temperature superposed viscoelastic moduli for a 6.7 wt % PSPI18−2C18M hybrid shown in Figure 3 exhibit unusual low-frequency behavior. Consistent with the addition of a solid dispersed phase, the moduli at all frequencies are higher for the hybrid as compared to the unfilled polymer.[21] We note that for this hybrid, and for all other hybrid concentrations, excellent time−temperature superposed master curves were obtained. Further, the frequency depen-

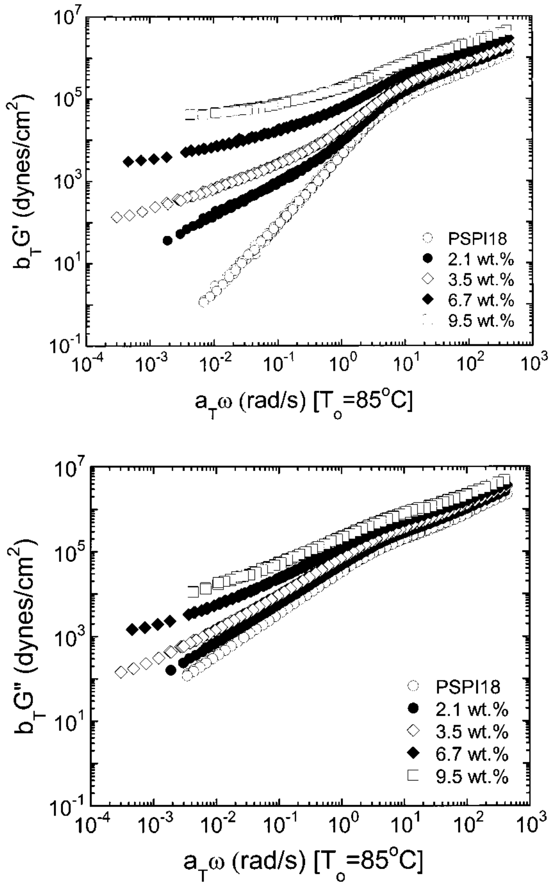

Figure 4. Time–temperature superposed linear storage modulus (a, top) and loss modulus (b, bottom) for the series of 2C18M-based PSPI18 intercalated hybrids. As expected, the moduli increase with increasing silicate loading at all frequencies. At high frequencies, the qualitative behavior of the storage and loss moduli are essentially unaffected. However, at low frequencies the frequency dependence of the moduli gradually changes from liquidlike to solidlike for nanocomposites with 6.7 and 9.5 wt % silicate.

dence of the high-frequency relaxation behavior in the hybrid is essentially unaffected by the addition of the filler, suggesting that the observed chain (and subchain) relaxation modes are unaltered by the presence of the layered-silicate. However, for $a_T\omega < 10$ rad/s, the viscoelastic response (especially G') for the hybrid displays a significantly diminished frequency dependence as compared to the unfilled PSPI18. In fact, G' becomes nearly independent of frequency at low $a_T\omega$ and exceeds G'', characteristic of a material exhibiting pseudo-solidlike behavior.

The dependence of the viscoelastic behavior on the layered-silicate concentration was investigated, and the master curves for the different hybrids are shown in Figure 4. The data for the 0.7 wt % silicate hybrid are almost identical to that obtained for the PSPI18 and are not shown in Figure 4. At all frequencies, both G' (Figure 4a) and G'' (Figure 4b) for the nanocomposites increase monotonically with increasing silicate loading. As noted earlier, the viscoelastic behavior at high frequencies ($a_T\omega > 10$ rad/s) is unaffected by the addition of the layered-silicate, with the exception of a monotonic increase in the modulus value. However, at low $a_T\omega$ (corresponding to a regime where the unfilled PSPI18 exhibits liquidlike behavior), both G' and G'' exhibit diminished frequency dependence, with the frequency dependence becoming weaker with increasing silicate content. For the 6.7 and 9.5 wt % nanocomposites in the low-ω region, G' exceeds G'' and G' is nearly independent of frequency, suggesting the possibility of pseudo-solidlike behavior for time scales at least of the order of 10^3–10^4 s.

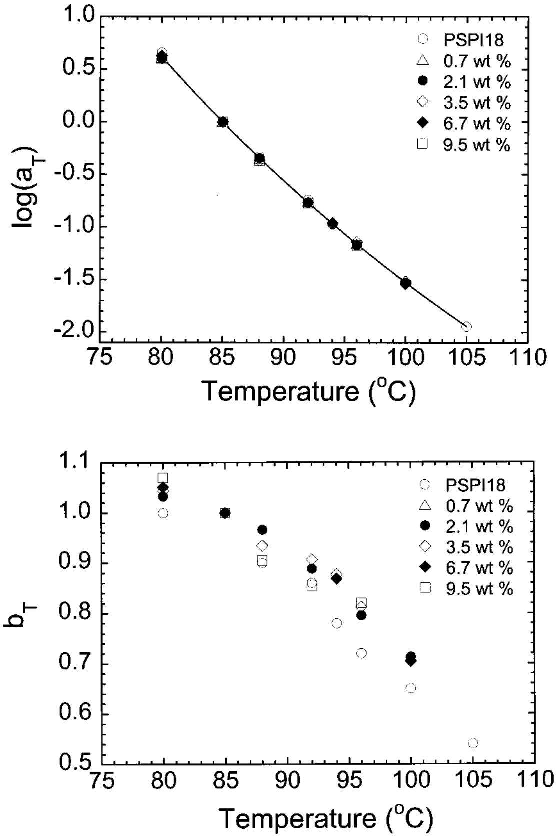

Figure 5. Frequency shift factors a_T (a, top) and Moduli shift factor b_T (b, bottom) for PSPI18 and the different hybrids studied in this work. The line shown in (a) is the best fit WLF equation (eq 4) to the a_T values for all the hybrids and the pure polymer.

The temperature dependence of the frequency and modulus shift factors (a_T and b_T) used to generate the master curves shown in Figures 2–4 are shown in Figure 5. The values of a_T are, within the errors of the experiment, independent of the silicate loading and well represented by a WLF relationship[20] given by

$$\log a_T = \frac{(-11.2 \pm 0.4)(T - T_0)}{(95 \pm 4) + (T - T_0)} \qquad (4)$$

where T_0 is the reference temperature, in this case 85 °C. The value of C_1 (where $\log a_T = [-C_1(T - T_0)]/[(C_2 + (T - T_0)])$ is consistent with that expected on the basis of the values of C_1 for PS and PI ($C_{1,\mathrm{PS}} = 22.5$ and $C_{1,\mathrm{PI}} = 2.8$ for $T_0 = 85$ °C)[22,23] and the known composition of the copolymer examined. The near independence of the frequency shift factors on the silicate loading suggests that the temperature-dependent relaxation processes observed in the viscoelastic measurements are essentially unaffected by the presence of the silicate layers. A substantial portion of the polymer is not intercalated between the layers of the silicate, and thus the temperature-dependent relaxation observed could be attributed to that of the matrix polymer. However, this does not imply that the relaxation behavior or the temperature dependence of the relaxation of the intercalated polymer or that near the surface of the layers is unaffected. The observed shift factors and the agreement with the principle of time–temperature superposition can easily be reconciled with the notion of two distinct populations of dynamical species: a matrix component that is unaffected and an intercalated or adsorbed component whose relaxation processes are much slower than the time scale of the experiments. Our experiments here are incapable of probing, if indeed such a distinct bimodal population exists, and only offer the insight that, for all the populations whose relaxation time change with temperature, the temperature dependence is identical to that of the pure polymer.

The b_T values required for time–temperature superpositioning of the linear viscoelastic data are large in magnitude and cannot be explained in terms of a simple density effect (i.e., $b_T = (\rho_0 T_0)/(\rho T)$, where ρ_0 and ρ are the densities at T_0 and T, respectively), where it would be expected that the values do not vary far from unity. These shift factors do not change significantly with silicate loading and are, within the errors of the experiments, comparable for all silicate loadings. One possible explanation for the substantial b_T values could be due to the block architecture of the polymer examined and the relative proximity of the order–disorder temperature to the temperature of the measurements. Although the polymer is disordered at all experimental temperatures, there exist substantial repulsive thermodynamic interactions between the PS and PI blocks, leading to considerable concentration fluctuations in the disordered state, whose magnitude diminish with increasing temperature.[24] Larson and Fredrickson[25] have suggested that, due to the increase in concentration fluctuations while approaching the order–disorder transition from the disordered state, there can be additional contributions to the moduli, and this might explain the magnitude of the vertical shift factors required. However, it is also expected that the principle of time–temperature superposition would fail if the magnitude of the corrections due to the concentration fluctuations to the moduli were substantial. It is possible that this failure of the principle of time–temperature superposition is subtle and thus not observable in our mechanical measurements.

(ii) Linear Stress Relaxation. To confirm the unusual viscoelastic behavior observed at low frequencies in the dynamic measurements for the layered-silicate-based hybrids, we have undertaken linear stress relaxation measurements, and the results of these are shown in Figure 6. The data reported here are in the linear regime, and the transition from linear to nonlinear behavior is described in a subsequent paper.[9] For any fixed time after the imposition of strain, the modulus increases with increasing silicate loading, similar to that observed in the dynamic viscoelastic measurements. Further, at short times (i.e., for $t < 0.5$ s), the stress relaxation behavior is qualitatively similar for all the hybrids and the unfilled polymer. At long times, however, the unfilled polymer relaxes like a liquid, while the hybrids with high silicate contents behave like a solidlike material for times as long as ~2000 s (at 85 °C).

The linear stress relaxation modulus is related to the dynamic oscillatory shear G' and G'' via the relaxation spectrum $H(\tau)$ as[20]

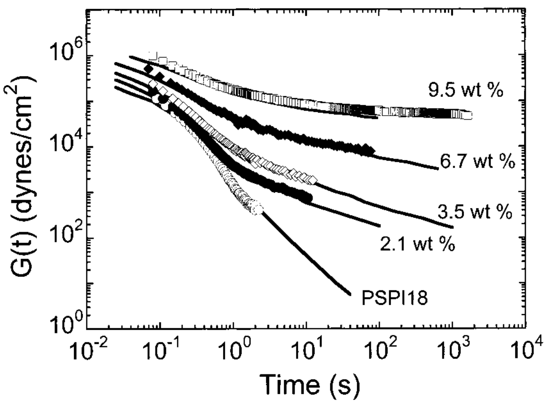

Figure 6. Linear stress relaxation measured modulus $G(t)$ at 85 °C for the unfilled PSPI18 and the hybrids. The weight fraction of the silicate in the hybrids is noted in the figure. Only 30% of the data collected are shown for all the data sets. The lines represent the predictions of eq 6 with the dynamic moduli presented in Figure 4. The agreement between the predictions and the measured data is excellent, suggesting the validity of eq 6 in describing the linear moduli for the hybrids.

$$G'(\omega) - G(t)|_{t=1/\omega} = \int_{-\infty}^{\infty}\left[\frac{\omega^2\tau^2}{1+\omega^2\tau^2} - \mathrm{e}^{-(1/\omega\tau)}\right]H\,\mathrm{d}(\ln\tau) \qquad (5)$$

Using a two-point collocation method, Ferry and co-workers[20,26] have shown that the transient $G(t)$ can be related to the corresponding dynamic moduli G' and G'' by

$$G(t) = G'(\omega) - 0.40G''(0.40\,\omega) + 0.014G''(10\omega)|_{\omega=1/t} \qquad (6)$$

This approximate relation has proven useful to relate the dynamic and transient moduli for homopolymers.[20] Recently, the same relationship was successfully used to describe the viscoelastic properties of micellar systems dispersed in a homopolymer.[27] On the basis of the dynamic viscoelastic response shown in Figure 4 and using eq 6, the modulus $G(t)$ was calculated and is shown in Figure 6. The agreement between the measured and the calculated values of $G(t)$ is excellent, suggesting that indeed the measurements in both dynamic oscillatory and stress relaxation mode are linear and that the approximate relation suggested by eq 6 is also valid.

On the basis of both the dynamic oscillatory shear and the stress relaxation moduli, it is clear that the addition of layered-silicate has a profound influence on the long time relaxation of the hybrids. With increasing silicate loading, the liquidlike relaxation observed for the unfilled polymer gradually changes to solidlike (or pseudo-solidlike) behavior for hybrids with silicate loadings in excess of 6.7 wt %. We discuss these features in the following section.

c. Phenomenological Explanation of Flow Behavior. The anomalous low frequency viscoelastic behavior can be attributed to at least two distinctly different mechanisms. First, the preferential attraction of the PS block to the silicate layers could cause the block copolymer to undergo an ordering transition, i.e., forming ordered microdomains. Previously, Green and co-workers[28] showed that thin films of a disordered PS–PMMA diblock copolymer can undergo an ordering transition when cast on silicon oxide substrates, a surface preferentially attractive to PMMA. It has also

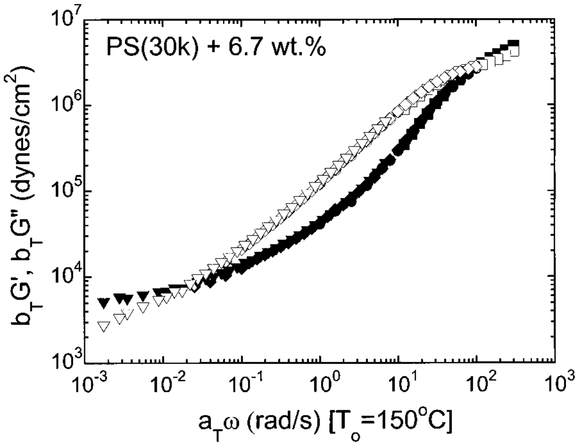

Figure 7. Time–temperature superposed mastercurves of the dynamic moduli for the PS (30K) + 2C18M-based 6.7 wt % silicate hybrid. The data were shifted to 150 °C. Open symbols correspond to b_TG'' while the filled symbols correspond to b_TG'. The remarkable similarity in the low-frequency behavior of this hybrid to that of the PSPI18 + 2C18M hybrid (6.7 wt % silicate) shown in Figure 3 suggests that the unusual viscoelastic properties observed for the PSPI18-based hybrids are not a result of a surface-induced ordering.

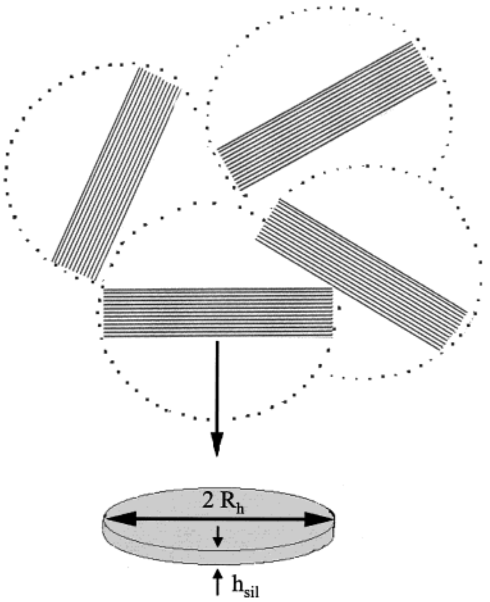

Figure 8. A schematic representation of the tactoids of layered silicates and their interaction with each other, resulting in incomplete relaxation of the hybrids.

been previously shown that, for ordered block copolymers, the low frequency response can be significantly diminished.[29] In particular, for materials with microstructures possessing cubic symmetry (such as spheres or gyroids) the low-frequency dependence of G' is nearly independent of frequency.

To address this possibility, the viscoelastic properties of a PS homopolymer ($M_w = 30$ k, $M_w/M_n < 1.06$) + 6.7 wt % 2C18M were investigated and are shown in Figure 7. Again, excellent time–temperature superpositioned master curves were generated, with the modulus shift factors not varying more than 3% from unity over the entire temperature range.[30] Comparing Figures 3 and 7 (the two hybrids have identical silicate loading), it is clear that the low-frequency viscoelastic behavior cannot be attributed to a surface induced ordering phenomenon, as the homopolymer-based hybrid is incapable of forming an ordered structure.

Alternatively, the low-frequency viscoelastic response can be explained in terms of a physical jamming of the dispersed layered silicates due to their highly anisotropic nature. The frequency dependence of the low-frequency G' and G'', wherein a pseudo-solidlike behavior is observed for the hybrids with 6.7 and 9.5 wt % silicate, is similar to that observed previously for end-tethered poly(ϵ-caprolactone)-based exfoliated nanocomposites.[7] There it was suggested that, due to the highly anisotropic nature of the layered silicates and simple geometric constraints, the layers would exhibit local correlations despite the hybrid being exfoliated. These local correlations cause the presence of domains, and the presence of these domains, similar to the studies of liquid crystalline and ordered block copolymer systems, caused the enhanced low-frequency modulus and the related low power-law dependence.[29]

We suggest that, in the intercalated nanocomposites examined here, the mesoscopic structure consists of silicate tactoids comprised of several tens of well-ordered layers (implied by the observation of at least three orders of Bragg reflections in the X-ray diffraction)[31] and the occasional presence of individual layers removed from the tactoids. Transmission electron micrographs of a hybrid formed with the same organically modified layered silicate and a polystyrene–poly(ethylene-*co*-butene-1) (PS–PEB) block copolymer revealed a mesoscopic structure consistent with the above picture and is shown elsewhere.[32] Further, a calculation of the domain size by the application of the Scherrer relationship to the X-ray diffraction data presented in Figure 1 (and not corrected for the instrumental broadening) suggests an average minimum tactoid size of ~15 nm and implying a minimum stacking of six layers in a tactoid.[31,33] On the basis of this mesoscopic structure and the underlying assumption that at low silicate concentrations the relative orientations of the tactoids are uncorrelated, we suggest that beyond a critical volume fraction the tactoids and the occasional individual layers are incapable of freely rotating and when subjected to small-amplitude shear are prevented from relaxing completely. This incomplete relaxation due to the physical jamming or percolation of the nanoscopic fillers leads to the presence of the pseudo-solidlike behavior observed in the 6.7 and 9.5 wt % hybrids. Further, we expect other viscoelastic signatures consistent with that of a percolated system (i.e., the presence of a yield stress, divergence of the viscosity with decreasing shear rate, etc.), and these are explored in a subsequent paper.[9]

To verify that the percolation of the stacks of layers (i.e., tactoids) is a plausible explanation, we estimate the percolation threshold for these hybrids parametrized in terms of the stack size. For this we consider a hypothetical hydrodynamic sphere surrounding each tactoid and consider the percolation of these hydrodynamic spheres to signify the onset of incomplete relaxation and the presence of pseudo-solid behavior in the hybrids (Figure 8). The percolation of random spheres in three dimensions has been calculated to occur for a volume fraction (ϕ_{per}) of ~0.30[34] and is only slightly changed by the inclusion of excluded-volume interactions. A simple volume filling calculation, assuming a uniform distribution of identically sized tactoids, yields a relationship between the critical tactoid size required (n_{per}, the number of silicate layers per tactoid) and the layered-silicate weight fraction at percolation ($w_{\mathrm{sil,per}}$) as

$$n_{\mathrm{per}} = \frac{4}{3\phi_{\mathrm{per}}}\left[\frac{w_{\mathrm{sil,per}}\,\rho_{\mathrm{org}}}{w_{\mathrm{sil,per}}\,\rho_{\mathrm{org}} + (1 - w_{\mathrm{sil,per}})\,\rho_{\mathrm{sil}}}\right]\frac{R_{\mathrm{h}}}{h_{\mathrm{sil}}} \qquad (7)$$

where R_{h} is the radius of the hydrodynamic volume (in this case equivalent to the radius of the disklike layered silicates), h_{sil} is the thickness of the silicate layers, and ρ_{org} and ρ_{sil} are the densities of the organic component and layered-silicate, respectively. Assuming that the silicate layers can be adequately represented by uniform disks of 0.5 μm diameter ($2R_{\mathrm{h}}$) and thickness 1 nm (h_{sil}), and assigning the weight fraction of silicate at the percolation threshold ($w_{\mathrm{sil,per}}$) to be 0.067 (pseudo-solid behavior is observed for the hybrids with 6.7 and higher weight percent layered-silicate), we obtain the average tactoid size to be ~30 layers. This average tactoid size is not unreasonable in light of the presence of several higher-order X-ray diffraction peaks and evidence from TEM measurements on hybrids of PS−PEB prepared with the same layered-silicate[32] which indicate that, in addition to a few delaminated layers, the tactoid size can range from 10 layers to over 50 layers. Further, this tactoid size implies that the effective anisotropy associated with the layered silicates is ~15−20. This aspect ratio is consistent with the calculation of geometrical percolation thresholds of overlapping oblate ellipsoids.[35] It is this anisotropy, along with the random relative arrangement of the tactoids, which leads to the observation of the percolation phenomenon at extremely low loadings of the silicate.

If, on the other hand, the tactoids were oriented preferentially in the shear direction, one would expect the tactoids to no longer form a percolated network structure and exhibit liquidlike flow behavior. It has been shown previously that, similar to other intrinsically anisotropic materials, these layered-silicate-based nanocomposites can also be shear aligned by the prolonged application of large-amplitude oscillatory shear.[7,8] The PSPI18 hybrids were subjected to similar prolonged large-amplitude oscillatory shear, during which the modulus initially decreased monotonically followed by saturation at a significantly lower value than the initial presheared modulus. The frequency dependence of the linear viscoelastic moduli for a 6.7 wt % 2C18M-based PSPI18 hybrid before and after prolonged oscillatory shear is shown in Figure 9. The data for 85 and 92 °C were obtained on samples shear aligned at the same temperature just prior to measurement of the frequency dependence in order to avoid artifacts that might be introduced due to disorientation of the aligned tactoids as a result of Brownian motion. On the basis of recovery measurements,[9] we believe this disorientation time to be ~20 000 s at 85 °C.

From Figure 9 it is clear that, for the aligned nanocomposite, in addition to the decrease in the absolute value of the modulus at all frequencies, the low-frequency behavior dependence is also significantly enhanced from the unoriented pseudo-solidlike behavior. This increased low-frequency dependence of the viscoelastic moduli suggests a breakdown of the percolated silicate network in the shear-aligned sample. In fact, for the case where the tactoids are aligned parallel to the shear direction, percolation would be expected when the effective two-dimensional disklike objects form a network. For the case of overlapping disks, on the basis of continuum model calculations, it is expected that percolation would occur at a volume fraction of disks of ~0.67.[34] For tactoids of ~30 layers this calculation would suggest a critical percolation threshold to occur at ~44 wt % of the layered silicate. We are currently pursuing measurements of delaminated or poorly ordered nanocomposites prepared with larger aspect ratio layered silicates, where it might be possible to observe the two-dimensional percolation at much lower loadings of silicate.

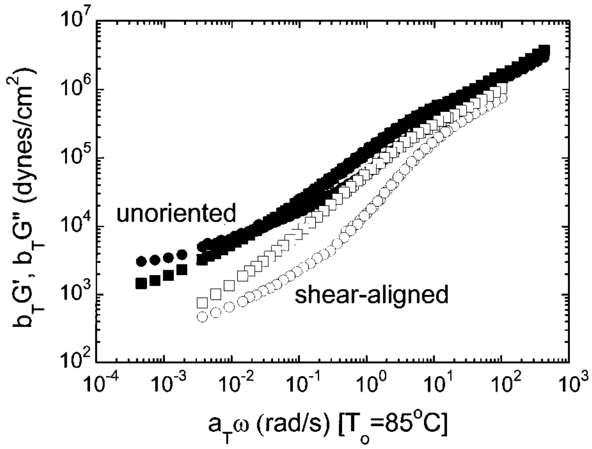

Figure 9. Effect of large-amplitude oscillatory shear on the linear viscoelastic moduli master curves (from data at 85 and 92 °C) for a PSPI18 + 2C18M hybrid (6.7 wt % silicate). Open symbols correspond to the shear-aligned sample while the filled symbols correspond to the unoriented sample, with the squares corresponding to *G*″ and circles corresponding to *G*′. The moduli decrease after shear alignment and have a dramatic effect on the low-frequency response with a more liquidlike behavior observable.

Concluding Remarks

We have investigated the melt-state linear viscoelastic behavior for a series of layered-silicate-based polymer nanocomposites. While the polymer studied here is a disordered diblock copolymer of polystyrene and polyisoprene, most of the conclusions of this work are independent of the architecture of the polymer and in fact are readily generalizable to low-molecular-weight homopolymers. The dynamic moduli and stress relaxation measurements suggest the presence of pseudo-solidlike behavior for hybrids with silicate loadings in excess of 6.7 wt %. We attribute this to the mesoscopic structure of randomly oriented silicate layer tactoids that form a three-dimensional percolated network structure at low silicate loadings due to the anisotropy associated with these tactoids. We have demonstrated that this pseudo-solidlike behavior is not associated with a possible ordering of the diblock copolymer at the silicate surface by reproducing the behavior in a homopolymer PS-based nanocomposite. Further evidence for this phenomenological explanation comes from the ability of large-amplitude oscillatory shear to shear align the tactoids and the concomitant decrease and change in the low-frequency behavior of the modulus. Several outstanding issues such as the nonlinear viscoelastic properties of these hybrids, effect of molecular weight of the matrix, the aspect ratio of the layered-silicate, and the strength of the silicate polymer interaction are yet to be understood. However, the linear viscoelastic properties appear to be most strongly correlated to the mesoscopic structure, and it is postulated that the molecular weight, interaction strength, etc., would most profoundly affect the mesostructure and hence the properties of these hybrids.

Acknowledgment. The authors thank Prof. Mohanty and Prof. Graessley for useful discussions. We would like to acknowledge financial support from the donors of the Petroleum Research Fund, administered by the American Chemical Society, and from the Texas Coordinating Board (ATP). This work made use of TCSUH/MRSEC Shared Facilities supported by the State of Texas through TCSUH and by NSF (DMR-9632667). We also thank Prof. Luss for the use of the TGA.

References and Notes

(1) Giannelis, E. P. *Adv. Mater.* **1996**, *8*, 29. Messersmith, P. B.; Giannelis, E. P. *Chem. Mater.* **1993**, *5*, 1064. Messersmith, P. B.; Giannelis, E. P. *J. Polym. Sci., Part A: Polym. Chem.* **1995**, *33*, 1047.

(2) Giannelis, E. P.; Krishnamoorti, R.; Manias, E. *Adv. Polym. Sci.* **1999**, *138*, 107.

(3) Krishnamoorti, R.; Vaia, R. A.; Giannelis, E. P. *Chem. Mater.* **1996**, *8*, 1728.

(4) Usuki, A.; Kojima, Y.; Kawasumi, M.; Okada, A.; Fukushima, Y.; Kurauchi, T.; Kamigaito, O. *J. Mater. Res.* **1993**, *8*, 1179. Kojima, Y.; Usuki, A.; Kawasumi, M.; Okada, A.; Fukushima, Y.; Kurauchi, T.; Kamigaito, O. *J. Mater. Res.* **1993**, *8*, 1185. Yano, K.; Usuki, A.; Okada, A.; Kurauchi, T.; Kamigaito, O. *J. Polym. Sci., Part A: Polym. Chem.* **1993**, *31*, 2493.

(5) Magauran, E. D.; Kieke, M. D.; Reichert, W. W.; Chiavoni, A. *NLGI Spokesman* **1987**, *50*, 453.

(6) Ramsay, J. D. F.; Lindner, P. *J. Chem. Soc., Faraday Trans.* **1993**, *89*, 4207. Ramsay, J. D. F.; Swanton, S. W.; Bunce, J. *J. Chem. Soc., Faraday Trans.* **1990**, *86*, 3919.

(7) Krishnamoorti, R.; Giannelis, E. P. *Macromolecules* **1997**, *30*, 4097.

(8) Krishnamoorti, R.; Giannelis, E. P. *Langmuir*, in press.

(9) Ren, J.; Silva, A. S.; Krishnamoorti, R. Manuscript in preparation.

(10) Vaia, R. A.; Giannelis, E. P. *Macromolecules* **1997**, *30*, 7990. Vaia, R. A.; Jandt, K. D.; Kramer, E. J.; Giannelis, E. P. *Macromolecules* **1995**, *28*, 8080.

(11) Vaia, R. A.; Giannelis, E. P. *Macromolecules* **1997**, *30*, 8000.

(12) Balazs, A. C.; Singh, C.; Zhulina, E. *Macromolecules* **1998**, *31*, 8370. Ginzburg, V. V.; Balazs, A. C. *Macromolecules* **1999**, *32*, 5681.

(13) Computer simulations have suggested that the phenyl groups of the intercalated PS chains exhibit a preference for the silicate surface due to the potential for development of strong interactions. Hackett, E.; Manias, E.; Giannelis, E. P. *J. Chem. Phys.* **1998**, *108* (17), 7410.

(14) Theng, B. K. G. *Formation and Properties of Clay-Polymer Complexes*; Elsevier: New York, 1979. Pinnavia, T. G. *Science* **1983**, *220*, 365.

(15) Lerner and co-workers[16] have demonstrated with PEO-based layered-silicate nanocomposites that the gallery height increases initially by 0.4 nm for hybrids with 15 wt % or less of PEO, and with increasing PEO a second d_{001} peak appears, suggesting an interlayer gallery height increase of 0.8 nm. Similar stepwise increases in gallery height have also been observed for small molecule intercalation of layered silicates[14] and has also been recently observed for PS-based nanocomposites.[17]

(16) Wu, J.; Lerner, M. M. *Chem. Mater.* **1993**, *5*, 835. Lemmon, J. P.; Lerner, M. M. *Chem. Mater.* **1994**, *6*, 207.

(17) Manias, E. D.; Giannelis, E. P. Unpublished results.

(18) Vaia, R. A.; Teukolsky, R. K.; Giannelis, E. P. *Chem. Mater.* **1994**, *6*, 1017.

(19) Fetters, L. J.; Lohse, D. J.; Milner, S. T.; Graessley, W. W. *Macromolecules* **1999**, *32*, 6847. Fetters, L. J.; Lohse, D. J.; Graessley, W. W. *J. Polym. Sci., Part B: Polym. Phys.* **1999**, *37*, 1023.

(20) Ferry, J. D. *Viscoelastic Properties of Polymers*; John Wiley & Sons: New York, 1980.

(21) Malkin, A. Y. *Adv. Polym. Sci.* **1990**, *96*, 69.

(22) Graessley, W. W. Physical Properties of Polymers.

(23) Gotro, J. T.; Graessley, W. W. *Macromolecules* **1984**, *17*, 2767.

(24) Lin, C. C.; Jonnalagadda, S. V.; Kesani, P. K.; Dai, H. J.; Balsara, N. P. *Macromolecules* **1994**, *27*, 7769.

(25) Larson, R. G.; Fredrickson, G. H. *Macromolecules* **1987**, *20*, 1897. Fredrickson, G. H.; Larson, R. G. *J. Chem. Phys.* **1987**, *86*, 1553.

(26) Ninomiya, K.; Ferry, J. D. *J. Colloid Sci.* **1959**, *14*, 36.

(27) Watanabe, H.; Yao, M.-L.; Sato, T.; Osaki, K. *Macromolecules* **1997**, *30*, 5905. Sato, T.; Watanabe, H.; Osaki, K.; Yao, M.-L. *Macromolecules* **1996**, *29*, 3881.

(28) Limary, R.; Green, P. F. *Macromolecules* **1999**, *32*, 8167.

(29) Fredrickson, G. H.; Bates, F. S. *Annu. Rev. Mater. Sci.* **1996**, *26*, 501. Larson, R. G.; Winey, K. I.; Patel, S. S.; Watanabe, H.; Bruinsma, R. *Rheol. Acta* **1993**, *32*, 245. Colby, R. H. *Curr. Opin. Colloids* **1996**, *1*, 454. Kossuth, M. B.; Morse, D. C.; Bates, F. S. *J. Rheol.* **1999**, *43*, 167.

(30) The b_T values ranged from 0.97 to 1.03 for the PS-based nanocomposites. This leads additional credence to the substantial b_T values observed for PSPI- and PSPI-based nanocomposites and suggests that the concentration fluctuations in those systems are responsible for the large b_T values.

(31) Brindley, G. W.; Brown, G. *Crystal Structures of Clay Minerals and Their X-ray Identification*; Mineralogical Society: London, 1980.

(32) Silva, A. S.; Tse, M. F.; Wang, H.-C.; Krishnamoorti, R. *Langmuir*, submitted.

(33) Warren, B. E. *X-ray Diffraction*; Dover Publications: New York, 1990. The Scherrer equation employed describes the crystallite or tactoid size l in terms of the full width at half-maximum of the 001 reflection (β), as $l = k\lambda/(\beta \cos \theta)$, where λ is the wavelength of the radiation, θ is half the diffraction angle, and k is a constant and is $\sim$0.94. For the X-ray diffraction data presented in Figure 1, $\lambda = 1.54$ Å, $2\theta \sim 2.55 \pm 0.2°$, and $\beta = 0.6 \pm 0.05°$, leading to a minimum average domain size l of 15 ± 1 nm.

(34) Isichenko, M. B. *Rev. Mod. Phys.* **1992**, *64*, 961.

(35) Garboczi, E. J.; Snyder, K. A.; Douglas, J. F.; Thorpe, M. F. *Phys. Rev. E* **1995**, *52*, 819.

MA992091U